NH_3-SCR of NO over a V-based Catalyst: Low-T Redox Kinetics with NH_3 Inhibition

Isabella Nova, Cristian Ciardelli, and Enrico Tronconi
Dipartimento di Chimica, Materiali e Ingegneria Chimica "G. Natta," Politecnico di Milano, I-20133 Milan, Italy

Daniel Chatterjee and Brigitte Bandl-Konrad
DaimlerChrysler AG Abteilung RBP/C, HPC: 096-E220, D-70546 Stuttgart, Germany

DOI 10.1002/aic.10939
Published online July 10, 2006 in Wiley InterScience (www.interscience.wiley.com).

We present transient kinetic data that demonstrate an inhibiting effect of ammonia on the NH_3-selective catalytic reduction (SCR) of nitric oxide (NO) at low temperatures over a V_2O_5-WO_3/TiO_2 commercial catalyst for vehicles. This effect has significant mechanistic as well as practical implications. It cannot be reproduced by conventional or modified Eley–Rideal approaches used in the past for SCR-deNOx stationary applications, but is well described by a novel dual-site redox rate expression assuming that ammonia may block the vanadium-related catalyst sites for NO + NH_3 activation. The same rate model also successfully represents the kinetic influence of the oxygen concentration. It is shown that account of ammonia inhibition at low temperatures is critical for simulating the highly transient operation of onboard SCR converters for diesel exhaust aftertreatment.
 AIChE J, 52: 3222–3233, 2006
Keywords: SCR deNOx, dynamic methods, ammonia inhibition, redox kinetics, diesel exhaust aftertreatment

Introduction

Selective catalytic reduction (SCR) with NH_3/urea is unanimously regarded as one of the most promising technologies for the abatement of NO_x emissions from vehicles[1]: in fact its commercialization, particularly for heavy-duty diesel engines, is being currently implemented in Europe to meet the emission limits associated with the EURO IV but also with the forthcoming EURO V regulations.[2-4] Indeed the design and development of SCR systems is a complex process involving the optimization of several parameters, like the urea dosing strategy, the position size and cell density of the SCR monolith catalyst, as well as the interaction between engine and aftertreatment system. In view of shortening development cycles and reducing development costs, it is very important to assess the performance of different setups and to understand the influence of different design parameters in an early stage. In this respect, the use of numerical simulations is a key factor: the transportation industry is therefore actively developing related engineering tools, such as SCR kinetic schemes and SCR converter models.

This task is facilitated in principle by the fact that the SCR technology is not new. NH_3-SCR over vanadia-type catalysts, wherein one molecule of NO is reduced by one molecule of ammonia in the presence of oxygen to give harmless dinitrogen and water, has represented for the last two decades the most effective commercial deNOxing process for stack gases from power plants and other stationary sources.[5] In this framework, the catalytic mechanism and kinetics of the SCR reaction have been extensively investigated[6]: the most commonly acknowledged mechanistic scheme is grounded on the assumption that only NH_3 is significantly adsorbed onto the catalyst, whereas NO reacts from the gaseous phase (or from a weakly adsorbed state) according to an Eley–Rideal (ER) mechanism. In the past, steady-state and transient kinetic data collected over V-based catalysts at conditions typical of stationary SCR appli-

Correspondence concerning this article should be addressed to E. Tronconi at enrico.tronconi@polimi.it.

cations (280°C $\leq T \leq$ 400°C) were successfully interpreted on the basis of the ER scheme.[5,6] However, mobile applications, where ammonia is supplied by decomposition of a urea solution, are much more demanding because they involve continuously transient operation in a much wider temperature window (150 °C $\leq T \leq$ 550°C): thus, it becomes critical to understand in detail the factors governing the SCR reaction rate over a broad range of conditions, and particularly at low temperatures, where simplified kinetics may have severe limitations when attempting to comply with strict emission regulations.

Inspection of the SCR scientific literature indicates several reports that are actually at variance with a simple single-site ER kinetic scheme under different respects.

Dumesic et al.[7] first showed that their steady-state SCR kinetic data over V-based catalysts were better described by a more complex approach including activation of adsorbed ammonia. Based on in situ FTIR and on-line mass spectrometry, they later proposed a catalytic cycle[8-11] associated with two different types of V-sites: (1) Brønsted acid sites, whereby NH_3 is adsorbed; and (2) surface redox sites, whereby ammonia is activated (oxidized) for reaction with NO, leading to partial reduction of the catalyst; closure of the cycle then involves reoxidation of these sites by gaseous oxygen. A microkinetic model reflecting such a three-step mechanism was able to describe steady-state SCR kinetic data.[11] Drawing from extensive investigations of the NH_3 SCR of NO over various supported vanadia catalysts examining the influence of V-coverage, nature of promoters and oxidic support, catalyst acidic and redox properties, and SCR reactivity, Wachs et al.[12] proposed that a dual-site mechanism is required for efficient deNOx over V-based systems: such a mechanism involves participation of both a surface vanadia redox site and an adjacent nonreducible acidic metal oxide site. An independent indication supporting the separation between ammonia "adsorption" sites and "reaction" sites was obtained by Lietti et al.[13] by transient experiments performed over model V_2O_5-WO_3/TiO_2 SCR catalysts: data at low temperature showed that a "reservoir" of adsorbed ammonia species is present on the catalyst surface and available for the reaction, possibly also associated with Ti- and W-bound ammonia species, whereas only V sites are responsible for the reactivity in the SCR reaction. Accordingly, two types of sites were postulated to exist on the catalyst surface, being responsible for different catalytic functions: NH_3 adsorption–desorption and NH_3 + NO reactivity. The transient kinetic data were fitted by a rate expression where the rate of the deNOx reaction depends on the global ammonia surface concentration only for NH_3 coverages below a characteristic "critical" value, corresponding to the fraction of active sites [modified θ_{NH_3} kinetics (Mθ)]. It was also shown that the need to invoke modified θ_{NH_3} kinetics vanishes at high temperatures, where the ammonia surface coverage is low and the usual ER approach becomes satisfactory.[13]

Another aspect apparently at variance with ER SCR kinetics is the fractional reaction order of NO documented by several authors[5,6]: even though other explanations are possible,[6] this may imply that, like ammonia, nitric oxide also reacts from an adsorbed state. Along these lines, Baiker et al.[14,15] proposed that the SCR reaction over a vanadia-based commercial catalyst proceeds by the ER mechanism at high temperatures, whereas a Langmuir–Hinshelwood (LH) mechanism prevails at low temperatures (<200°C). The same authors confirmed weak NO adsorption over the vanadia/titania catalyst by thermoanalytical methods combined with mass spectroscopy.[15] Valdés-Solìs et al.[16,17] recently observed that adsorption of NO is not negligible over V-based carbon-supported catalysts at low temperatures (125–175°C), and provided both temperature-programmed desorption (TPD) and kinetic evidence in favor of a Langmuir–Hinshelwood mechanism involving reaction between NO and NH_3 both adsorbed on two different types of catalyst centers. In this case, however, the carbon-based support may also play a significant role.

A remarkable but less commonly recognized aspect conflicting with the ER mechanism is the inhibiting effect of NH_3 on the SCR rate observed at low temperatures by various authors[18-22] over both V-based and other mixed-oxide catalysts. Such an effect is hardly compatible with a simple ER approach: it has been interpreted as evidence that NH_3 adsorbs competitively onto the same type of sites as those on which NO is activated.[19] Notably, accurate description of this effect is important for the design of mobile exhaust after treatment devices, which are often required to operate in the temperature (T) range around 200°C, that is, at significantly lower temperature levels than in stationary SCR applications, and under transient conditions with respect to ammonia concentration as a result of the urea injection strategy.[23]

As a final point, the Eley–Rideal scheme neglects the kinetic influence of oxygen: it has been reported that, from a practical perspective, this simplification is typically acceptable for O_2 concentrations in excess of 1–2% v/v, given that the rate of the SCR reaction becomes almost independent of the oxygen feed content above this level.[5] Nonetheless, because exhaust gases contain oxygen, and oxygen is involved in the SCR chemistry, a relevant reaction model should reflect oxygen participation: it is generally agreed in fact that oxygen is needed for reoxidation of the catalyst according to a Mars–van Krevelen or redox-type mechanism.[5] Moreover, it is also agreed that at low temperature the catalyst reoxidation by gas-phase oxygen is the rate-determining step of the overall reaction[14,24,25]: for example, Marshneva et al.[26] found that over their V-based catalysts the activation energy of the SCR reaction was equal to the activation energy of vanadia reoxidation. Surprisingly, however, only a limited number of SCR rate equations have been proposed so far that contain an O_2 dependency derived according to a redox mechanism.[5] Again, in view of the low-temperature operation of SCR exhaust aftertreatment devices, appropriate consideration of the O_2 dependency, being associated with the rate-limiting step of the catalytic process, seems of great practical interest for applications to vehicles.

To clarify the significance of all these aspects, herein we investigate by dynamic methods the transient kinetics of the NO + NH_3 SCR reaction over a commercial V_2O_5–WO_3/TiO_2 catalyst for mobile applications, specifically addressing the ammonia inhibition at low temperatures as well as the oxygen influence. We also derive an original *modified redox* (MR) rate expression for the NO + NH_3 SCR reaction, which essentially reconciles all of the above-mentioned mechanistic features. The kinetic model is fitted to the transient data and the results are compared with fits of the same data based both on standard Eley–Rideal kinetics and on modified θ_{NH_3} kinetics.[13] Finally, the implications of our results are discussed in relation both to

fundamental aspects of the SCR catalytic chemistry and to practical issues in vehicle exhaust gas aftertreatment.

The present work is part of a fundamental and applied study of the NO–NO_2/NH_3/O_2 reacting system in view of the development of integrated exhaust aftertreatment devices for mobile applications.[23,27-31] Only the NO + NH_3 (designated Standard) SCR reaction is addressed herein: the kinetics of the so-called Fast SCR reaction, involving both NO and NO_2 as reactants in addition to ammonia, is currently being investigated in conjunction with its complex catalytic mechanism[28,30,31] and will be reported in a forthcoming article.

Methods

Experimental procedures

For the purposes of the present study, dedicated unsteady kinetic SCR experiments of various nature were performed in the 50–450°C *T*-range over a commercial V_2O_5–WO_3/TiO_2 catalyst with medium-high V-content, originally supplied by DaimlerChrysler as an extruded honeycomb monolith. The monolith catalyst was crushed and ground to powder (140–200 mesh); a sample of powder (160 mg) was diluted with 80 mg of quartz and loaded in a flow-microreactor consisting of a quartz tube (ID = 6 mm) directly connected both to a UV analyzer (ABB Limas 11-HW) and to a quadrupole mass spectrometer (Balzers QMS 200), which operated in parallel.

The dynamics of the NH_3 + NO SCR reaction were investigated using the *transient response method* (TRM),[13] that is, by performing step changes of the NH_3 feed concentration ($0 \rightarrow 1000 \rightarrow 0$ ppm) at constant NO feed content (1000 ppm) in the presence of water (1% v/v) and oxygen (2 and 6% v/v). The system was operated at atmospheric pressure with a gas hourly space velocity (GHSV) equal to 9.2×10^4 h^{-1}. In each experiment the UV analyzer provided the temporal evolution of the outlet NO, NO_2, and NH_3 concentrations. Helium was used as carrier gas, so that nitrogen, which is the main SCR product, could be detected by the mass spectrometer (MS), thus allowing the evaluation of overall N-balances, which always closed within ±5% at steady state. As a consistency check, the outlet concentration traces of NO and NH_3 were also estimated from the MS signals after suitable calibration: the steady-state levels agreed satisfactorily with those measured by the UV analyzer, whereas the transient phases were typically associated with a slower response, particularly for NH_3. Therefore, only the outlet concentration traces of NH_3 and NO generated by the UV analyzer were considered for the dynamic kinetic analysis reported in this work, in combination with the N_2 trace from the MS.

In addition to TRM runs, *temperature-programmed reaction* (TPR) experiments were also performed to study the response of the SCR system to temperature variations. In this case NH_3 (1000 ppm) + NO (1000 ppm) with O_2 (2 or 6% v/v), H_2O (1%), and balance He were initially fed at 50°C and then the catalyst temperature was continuously increased at 2 K/min up to 450°C.

Diagnostic preliminary tests showed no significant oxidation of NO to NO_2 up to 450°C: accordingly, the data herein presented reflect the reactivity of NO + NH_3 + O_2 only (Standard SCR).

Intraparticle gradients and gas–solid mass transfer limitations were ruled out by theoretical diagnostic criteria.[32]

Kinetic analysis

The transient data collected over the powdered SCR catalyst were analyzed according to a dynamic one-dimensional isothermal isobaric heterogeneous plug-flow model of the test microreactor[27] to obtain estimates of the relevant SCR rate parameters.

To fully describe the NH_3–NO/O_2 reacting system in the whole *T*-range from 50 to 450°C, NH_3 adsorption–desorption, NH_3 oxidation, and SCR deNOx reaction have to be considered, that is:

$$NH_3 \Leftrightarrow NH_3^* \tag{R1}$$

$$4NH_3^* + 3O_2 \rightarrow 2N_2 + 6H_2O \tag{R2}$$

$$4NH_3^* + 4NO + O_2 \rightarrow 4N_2 + 6H_2O \tag{R3}$$

Accordingly, the test reactor model constitutes the mass balances of adsorbed NH_3 and of gaseous NH_3, NO, and N_2, as reported in the following:

*Adsorbed Phase: NH_3**

$$\Omega \frac{\partial \theta_{NH_3}}{\partial t} = r_{ads} - r_{des} - r_{ox} - r_{NO} \tag{1}$$

Gas Phase: NH_3, NO, and N_2

$$\varepsilon \frac{\partial C_{NH_3}}{\partial t} = -v \frac{\partial C_{NH_3}}{\partial z} - (1-\varepsilon)(r_{ads} - r_{des}) \tag{2}$$

$$\varepsilon \frac{\partial C_{NO}}{\partial t} = -v \frac{\partial C_{NO}}{\partial z} - (1-\varepsilon) r_{NO} \tag{3}$$

$$\varepsilon \frac{\partial C_{N_2}}{\partial t} = -v \frac{\partial C_{N_2}}{\partial z} + (1-\varepsilon)(r_{NO} + 1/2 r_{ox}) \tag{4}$$

The set of partial differential equations (PDEs; Eqs. 1–4), with obvious initial and boundary conditions, was solved numerically according to the method of lines, based on axial discretization with backward finite differences and on time integration by Gear's algorithm.

To account for the delayed NH_3 evolution, Eq. 2 was coupled with an empirical model describing the ammonia response function of the rig and of the analyzers. Blank ammonia step change experiments (not shown) were used to fit the NH_3-delay model, which consisted of two continuous stirred tanks in parallel.

Concerning the rate expressions, nonactivated NH_3 adsorption and Temkin-type NH_3 adsorption–desorption kinetics were adopted, in line with previous findings[13,18]:

$$r_{ads} = k_{ads} C_{NH_3} (1 - \theta_{NH_3}) \tag{5}$$

$$r_{des} = k_{des}^{\circ} \exp\left[-\frac{E_{des}^{\circ}}{RT} (1 - \alpha \theta_{NH_3}) \right] \theta_{NH_3} \tag{6}$$

It should be emphasized that build-up/depletion of adsorbed ammonia onto the catalyst surface is the slow process controlling the overall dynamics of the SCR reaction over V-based catalysts,[13,22] with characteristic times of the order of minutes. In comparison, the reactive processes involving nitric oxide exhibit virtually instantaneous dynamics.

At the highest investigated temperatures ammonia oxidation (Reaction R2) was also observed, its rate being herein empirically fitted by

$$r_{ox} = k^{\circ}_{ox}\exp\left(-\frac{E_{ox}}{RT}\right)\theta_{NH_3}\left(\frac{p_{O_2}}{0.02}\right)^{\beta} \quad (7)$$

For the NO + NH_3 SCR (Reaction R3), three different rate laws were implemented and compared in this work: they are presented and discussed in the following paragraphs.

The kinetic parameters for ammonia adsorption–desorption, in Eqs. 5 and 6, and for ammonia oxidation, in Eq. 7, were estimated in previous work by regression on TRM, TPD, and TPR runs performed with feeds including only NH_3 in the presence of O_2 and water.[23,27] Likewise, an independent estimate of the NH_3 adsorption capacity Ω was obtained from NH_3 adsorption isotherms at low temperature.[23] The same estimates were retained in this work with no further adjustment. Corresponding parameter values are reported in Chatterjee et al.[23]

As presented in the following, the rate parameters appearing in the three alternative rate expressions for the SCR reaction herein considered have been estimated in this work by global multiresponse nonlinear regression of TRM and TPR runs performed with feeds including both NH_3 and NO in the presence of water (1% v/v) and oxygen (2 and 6% v/v), taking the temporal evolutions of the outlet NH_3, NO, and N_2 concentrations as the fitted responses: a robust multimethod regression routine was used for this purpose.[33,34] Additional dedicated *T*-ramp experiments showed a negligible effect of the H_2O feed content $> 1\%$ v/v.

Transient Experiments

Kinetic runs at 2% O_2

Figure 1 (A, B, or C, symbols) displays selected step-response TRM experiments performed with 2% O_2 at different temperatures (200, 225, 250, and 275°C), in terms of NH_3, NO, and N_2 outlet concentrations vs. time.

In the run performed at $T = 250$°C (squares), upon NH_3 step feed at $t = 0$ s the NH_3 outlet concentration trace exhibited a dead time ($\approx$250 s) and then slowly grew with time on stream, eventually approaching a steady-state value of about 200 ppm, which is much lower than the ammonia feed concentration level (1000 ppm). In correspondence to the NH_3 admittance to the reactor, a sudden drop of the NO outlet concentration was observed together with a mirror-like increment of the N_2 concentration, associated with the start-up of the SCR reaction. The levels of NH_3, NO, and N_2 at steady state were in fact consistent with the stoichiometry of the standard SCR reaction (R3), with a conversion close to 80%. After shutdown of the ammonia feed ($t = 1500$ s) the concentrations of NH_3, NO, and N_2 slowly recovered their feed levels, as all the ammonia still adsorbed on the catalyst surface was progressively depleted by the reaction with nitric oxide.

The dynamic features above described are common to all the experiments performed in the high-temperature range (>250°C): Figure 1 (A, B, or C, diamonds) also shows, for instance, the run at 275°C, at which temperature almost complete steady-state conversion of the reactants was approached.

On the other hand, the experiments performed at lower temperatures, that is, 225°C (Figures 1A, 1B, or 1C, triangles) and 200°C (circles), exhibited a different dynamic behavior of NO and N_2 during both the NH_3 start-up phase and the NH_3 shut-off transient. The more significant effect was observed when the NH_3 feed concentration was restored to 0 ppm ($t = 1500$ s): the NO outlet concentration first decreased, passed through a minimum, and then began to increase as a result of the depletion of adsorbed ammonia. A symmetrical evolution was observed for N_2, thus proving that during the transient phase of ammonia shutdown, when only adsorbed NH_3 was reacting with NO continuously fed to the reactor, the deNOx activity of the system was temporarily enhanced until complete depletion of the residual NH_3 on the catalyst surface. This evidently confirms that excess ammonia inhibits the SCR reaction, as already indicated by other authors.[18-22]

A minor transient feature was also manifest when ammonia was admitted to the reactor ($t = 0$ s): the NO outlet concentration immediately decreased, went through a weak minimum near 150 s, and finally slightly increased, reaching steady state corresponding to the end of the ammonia feed phase ($t \approx 2800$ s). Again, the nitrogen evolution was symmetrical to that of NO. The same ammonia inhibition effect, invoked to explain the enhancement in the deNOx conversion at ammonia shutdown, can also explain this transient behavior. In fact both features suggest the existence of an optimal ammonia surface concentration, which is lower than the coverage established at steady state.

It is worth noting that such transient effects arising from NH_3 inhibition were most evident at the lowest investigated temperature (200°C), but gradually vanished on increasing the reaction temperature (that is, reducing the amount of adsorbed NH_3 present on the catalyst surface) and were no longer visible at $T \geq 250$°C.

Implications of NH_3 inhibition

Different mechanistic proposals can be tentatively put forward to interpret the observed low-temperature–inhibiting action of NH_3.

A first explanation, along the lines of the commonly accepted high-*T* SCR chemistry, involves the possible adsorption of excess ammonia onto NH_3 already adsorbed on the catalyst centers. Indeed, the formation of "dimeric" ammonia adspecies at high NH_3 coverages was recently detected by IR spectroscopy over H-ZSM5.[35] It is expected that such a process may block the activation of NH_3 and its interaction with NO, thus partially suppressing SCR reactivity. This conjecture is compatible with NO reacting from the gas phase with ammonia on a single catalytic site, but introduces additional complexity compared to that of a conventional ER approach.

On the other hand, the observed NH_3 inhibition can also be rationalized according to a classic Langmuir–Hinshelwood (LH) mechanism, that is, invoking a competition between NO and NH_3 for adsorption onto the same catalytic site. It is apparent from Figure 1, in fact, that during the NH_3 shutdown

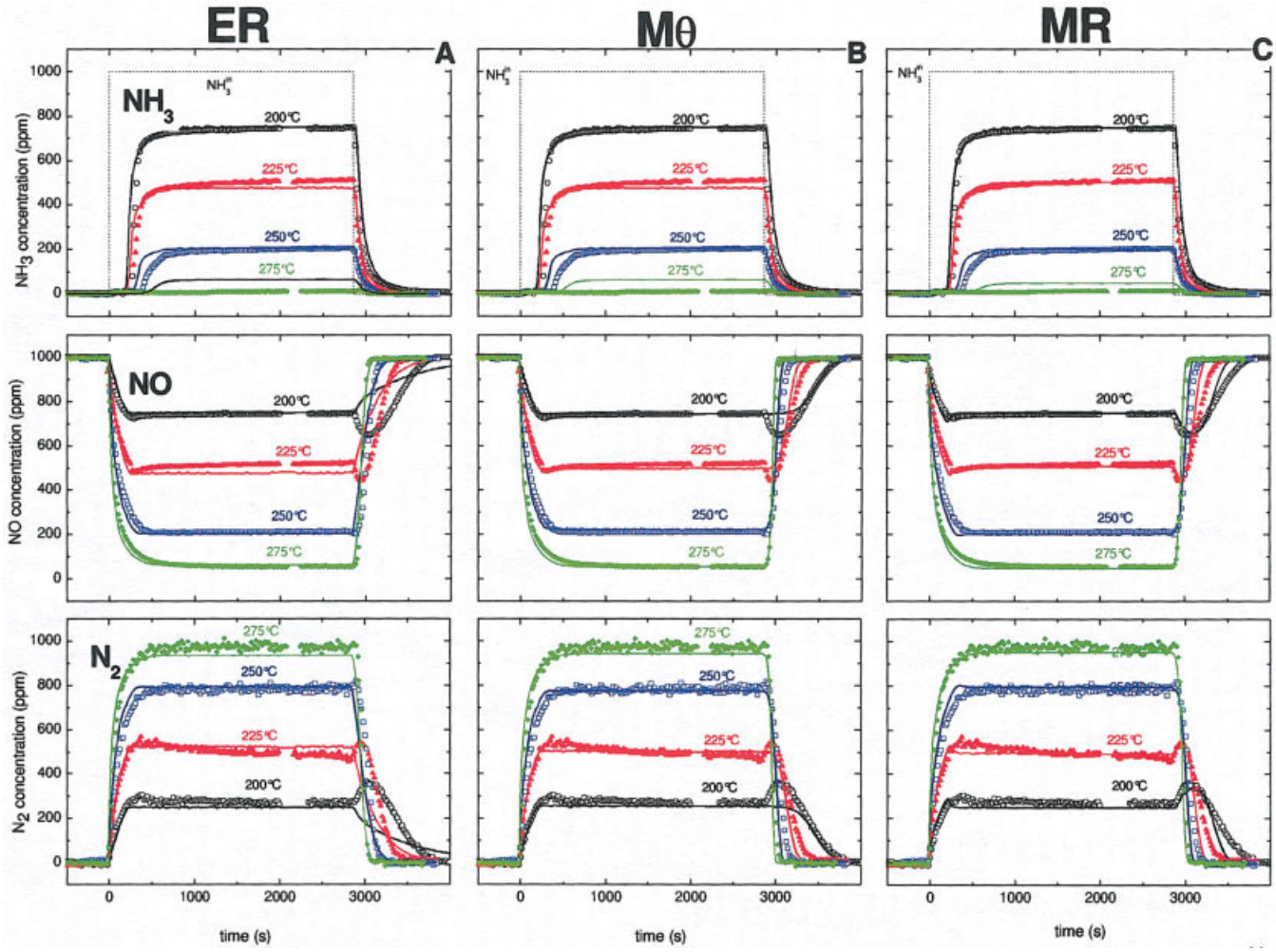

Figure 1. Transient selective catalytic reduction (SCR) microreactor experiments with step feed of NH_3 (0–1000 ppm) in NO (1000 ppm) + O_2 (2% v/v) and H_2O (1% v/v) + He at different temperatures.

Symbols (A, B, C): measured concentrations of NH_3, NO, N_2 at reactor outlet. Lines ER: kinetic fit using the Eley–Rideal rate law (Eq. 8). Lines Mθ: kinetic fit using the modified θ_{NH_3} rate law (Eq. 9). Lines MR: kinetic fit using the modified redox rate law (Eqs. 16 and 17). [Color figure can be viewed in the online issue, which is available at www.interscience.wiley.com]

transients the SCR rate was enhanced when both gaseous and adsorbed NH_3 concentrations were lower than those at steady state: this suggests that the incremented deNOx efficiency may have resulted from improved adsorption of NO onto the catalyst active sites as a result of the reduced NH_3 concentration level. It is commonly agreed that NO hardly adsorbs onto oxidized V-based SCR catalysts.[6] There are exceptions,[15-17] however, and important NO adsorption has been reported on several other oxide-based systems active in SCR catalysis.[6] In any case, the lack of clear evidence for individual NO adsorption in significant amounts does not necessarily rule out that NO can be activated by the catalyst under reactive conditions in the presence of ammonia/oxygen. A low activation energy pathway for the SCR reaction over zeolite catalysts was recently proposed, based on in situ FTIR spectroscopy and isotopic labeling studies, which involves the activation of NO on catalytic oxidative sites to form nitrite species: these would then react rapidly with NH_3 to give $N_2 + H_2O$ via ammonium nitrite as an unstable intermediate.[36,37] In this respect it is worth mentioning that strong ammonia inhibition is well known in the case of the SCR reaction over zeolite catalysts, negative NH_3 reaction orders having been reported by several authors.[6,38-40]

Finally, according to a third alternative explanation of NH_3 inhibition, one can speculate, in line with a dual-site approach, that the NO + NH_3 SCR rate-limiting step, occurring on V-sites and involving a redox catalyst function, may be adversely affected by NH_3 adsorbed onto nearby acidic sites, due to electronic interaction or possibly direct blocking of the redox sites.

In addition to significant mechanistic implications, however, the low-T NH_3 inhibition effect also has remarkable practical consequences. On-board operation of SCR converters for vehicles necessarily involves fast dynamics in the low-temperature range, associated with high-frequency NH_3 (urea) injections, such as that included in standard ETC cycles.[23] Under such highly transient conditions, the performances of the SCR converter are governed by the same dynamic features apparent during the NH_3 shutdown phase of the TRM run at 200 °C in Figure 1. Thus, inclusion of such effects in a relevant kinetic model is clearly of interest for the industrial implementation of the SCR technology on vehicles.

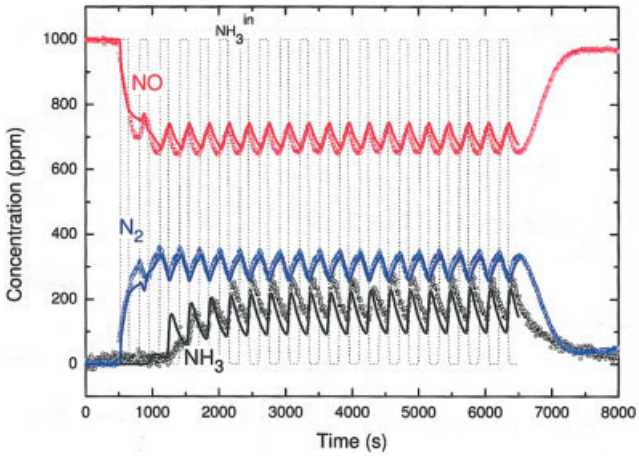

Figure 2. Transient SCR microreactor experiments with high-frequency NH_3 feed pulses (1000 ppm) in flowing NO (1000 ppm) + O_2 (2% v/v) and H_2O (1% v/v) + He at 200°C.

Symbols: outlet concentration of ammonia (circles), NO (squares), and N_2 (triangles). Dotted lines: feed ammonia concentration. Solid lines: simulation using the MR rate law (Eqs. 16 and 17). [Color figure can be viewed in the online issue, which is available at www.interscience.wiley.com]

Accordingly, to better analyze the ammonia inhibition effect under conditions closer to those of mobile SCR applications we have collected more transient kinetic data by performing high-frequency NH_3 feed pulses ($0 \rightarrow 1000$ ppm $\rightarrow 0$) in a stream of 1000 ppm of NO, 2% O_2, and 1% H_2O + He at different temperatures. Figure 2 shows, for example, the results at 200°C: herein pulses have been generated by cycling subsequent phases (150 s each) with and without ammonia. The experimental data exhibit the same characteristic transient behavior already observed for the longer transient experiments at low T (Figure 1, symbols): a maximum in the NO conversion was reached during each pulse after the NH_3 shutdown, in agreement with the aforementioned ammonia inhibition effect. Accordingly, the average NO conversion measured during this series of fast ammonia pulses (that is, about 32%) resulted in a somewhat higher value than the steady-state level achieved during one single ammonia pulse at the same reaction conditions (NO conversion $< 30\%$).

Kinetic runs at 6% O_2

Transient kinetic experiments were also performed in the presence of a higher concentration of oxygen: 6% v/v. Results collected at different temperatures are displayed in Figure 3 (symbols) in terms of NH_3, NO, and N_2 outlet concentration traces vs. time (T = 200, 225, 250, 275°C). They are qualitatively similar to those with 2% v/v oxygen feed in Figure 1 and discussed above. Particularly, two different behaviors of the NO and the N_2 concentration traces were again observed when the NH_3 feed was opened up/shut down. In the high-T range, monotonic temporal evolutions were observed: at NH_3 shutdown they slowly recovered their feed levels, using up the ammonia still adsorbed on the catalyst surface. In the low-T range, again maxima–minima behaviors became apparent: thus, at ammonia shutdown the NO concentration (and symmetrically the N_2 production) decreased at first, went through a minimum, then began to increase and approached its steady-state value. Thus, the higher oxygen content did not alter the dynamic features of the transient experiments and, in particular, the ammonia inhibiting action was still evident to a similar extent, especially at ammonia shutdown.

The main effect of the higher oxygen concentration was a slight enhancement of the SCR conversion, as measured by the steady-state levels of ammonia, NO, and nitrogen: for example, at 250°C, 780 ppm of nitrogen was measured at steady state when 2% oxygen was fed to the reactor (see Figure 1), whereas in the presence of 6% of oxygen the SCR reaction produced 820 ppm of nitrogen (see Figure 3).

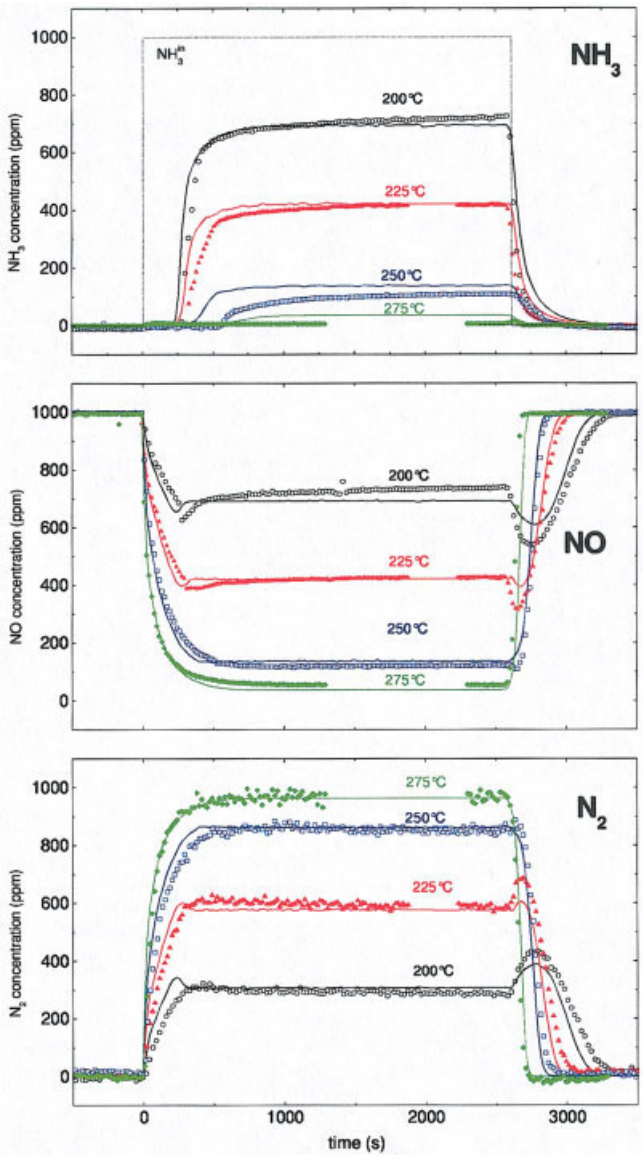

Figure 3. Transient SCR microreactor experiments with step feed of NH_3 (0–1000 ppm) in NO (1000 ppm) + O_2 (6% v/v) and H_2O (1% v/v) + He at different temperatures.

Symbols: measured concentrations of NH_3 (circles), NO (squares), and N_2 (triangles) at reactor outlet. Lines: kinetic fit using the MR rate law (Eqs. 16 and 17). [Color figure can be viewed in the online issue, which is available at www.interscience.wiley.com]

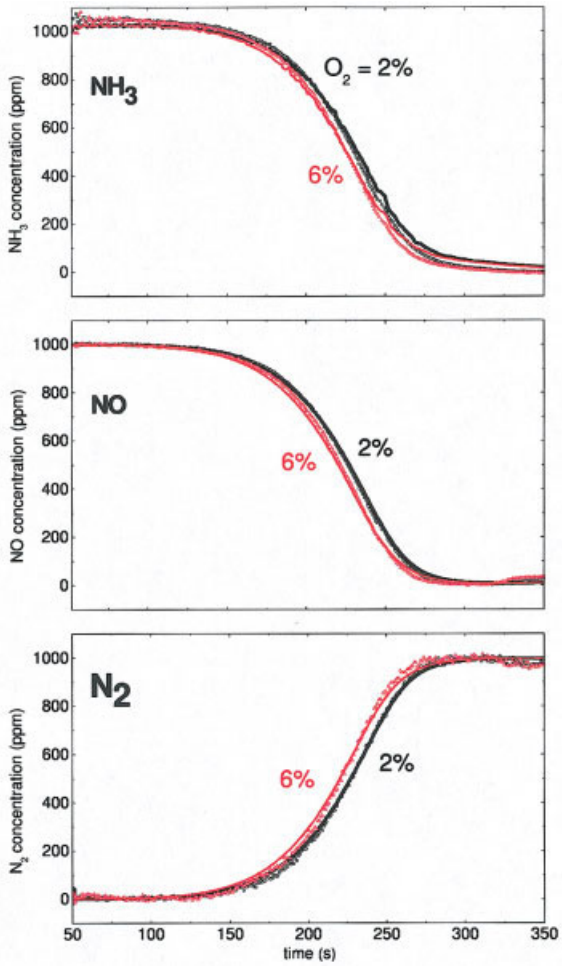

Figure 4. NO (1000 ppm) + NH_3 (1000 ppm) temperature-programmed reaction (TPR) runs O_2 (6% v/v) and H_2O (1% v/v) + He; heating rate = 2 K/min.

Symbols: measured concentrations of NH_3, NO, and N_2 at reactor outlet. Lines: kinetic fit using the MR rate law (Eqs. 16 and 17). [Color figure can be viewed in the online issue, which is available at www.interscience.wiley.com]

The kinetic effect of oxygen was further studied by performing *T*-ramps (TPR runs) with both 2 and 6% v/v O_2 in the feed stream: Figure 4 compares the corresponding outlet concentration traces of NH_3, NO, and N_2 vs. catalyst temperature: a moderate promoting effect of oxygen on the SCR activity was again clearly apparent over the whole investigated *T*-range. With both O_2 feed contents, ammonia and nitric oxide were consumed, starting from about 150°C to form stoichiometric amounts of N_2, and reached 100% conversion around 300°C. No other reaction products were formed even at the highest investigated temperatures (up to 450°C). The activity results obtained in the NH_3 + NO reaction during the *T*-ramps closely matched the steady-state values in the transient experiments presented in Figures 1 and 3: for example, during the TPR run at 250°C the NO conversion measured when feeding 2% of oxygen was roughly 75%, which well compares with the NO outlet concentration (220 ppm) measured during the corresponding TRM run.

Kinetic Analysis

Rate expressions and kinetic fit at 2% O_2

The kinetic analysis of the whole set of transient data collected over the powdered SCR catalyst has been addressed using the dynamic one-dimensional isothermal heterogeneous plug-flow model of the test microreactor[23] described earlier under Methods (Eqs. 1–7).

To challenge different mechanistic proposals for SCR catalytic kinetics on a quantitative basis, three rate expressions for the SCR reaction have been examined: they are discussed herein particularly in relation to their ability to reproduce the dynamic features of our experiments.

1. Eley–Rideal (ER) Kinetics. In line with several literature indications,[5,6] we started from a standard Eley–Rideal (ER) rate law,[13,21,27] assuming that the SCR reaction occurs between adsorbed ammonia and gaseous (or weakly adsorbed) NO:

$$r_{NO} = k^{\circ}_{NO} e^{(-E^{\circ}_{NO}/RT)} C_{NO} \theta_{NH_3} \tag{8}$$

A global multiresponse nonlinear regression of the five TRM and TPR runs performed with 2% v/v O_2 provided the estimates of the two rate parameters in Eq. 8 (k°_{NO}, E°_{NO}) reported in Table 1: their orders of magnitude are consistent with previous literature reports.[13,18]

The data fits obtained using ER kinetics (Eq. 8) are compared in Figure 1A (solid lines) with the TRM data at 2% oxygen. In all cases a satisfactory agreement was achieved between experimental and calculated data, except for the NH_3 start-up and shutdown transients at the lowest investigated temperatures: in these cases, the minima in the NO concentration trace and the corresponding maxima in the N_2 trace were not reproduced by the model. This is not surprising, given that Eq. 8 does not take into account the inhibiting effect of NH_3 on the SCR reaction to which such a nonmonotonic behavior is ascribed.

2. Modified θ_{NH_3} (Mθ) Kinetics. In previous works,[13,22] a modified ER rate expression was used [modified θ_{NH_3} (Mθ)] to describe transient data collected at low temperatures, indicating that a "reservoir" of NH_3 species, possibly adsorbed on poorly reactive but abundant W and Ti acidic sites, is present and available for the SCR reaction upon ammonia desorption followed by readsorption at the active V sites:

$$r_{NO} = k^{\circ}_{NO} e^{-E^{\circ}_{NO}/RT} C_{NO} \theta^{*}_{NH_3} (1 - e^{-\theta_{NH_3}/\theta^{*}_{NH_3}}) \tag{9}$$

Table 1. Orders of Magnitude of the Parameter Estimates for the Three Investigated SCR Rate Laws

	ER Eq. 7	Mθ Eq. 8	MR Eqs. 16 and 17
k°_{NO} (1/s)	1.8×10^{11}	1.4×10^{10}	7.0×10^{7}
E°_{NO} (kJ/mol)	93	74	55
$\theta^{*}_{NH_3}$	—	7.3×10^{-2}	—
K_{NH_3}	—	—	1.5
k_{O_2} (m^3 $bar^{1/4}$/mol)	—	—	86
k_{sp} (1/s)	—	—	4.8×10^{-2}

Equation 9 implies that r_{NO} becomes essentially independent of the ammonia surface coverage above a critical NH_3 coverage identified by $\theta^*_{NH_3}$.

Just as for the ER rate expression, a global multiresponse nonlinear regression of all the TRM and TPR runs performed with 2% O_2 provided the estimates of the three rate parameters in Eq. 9 (k°_{NO}, E°_{NO}, $\theta^*_{NH_3}$) listed in Table 1.

Figure 1B (solid lines) shows the fit obtained using Eq. 9 for the TRM data with 2% oxygen. It is apparent that this kinetic expression affords a good agreement between experimental and calculated data, again with the exception of the outlet concentrations of nitric oxide and nitrogen during the NH_3 start-up and shutdown transients at the lower temperatures, where it predicts a prolonged duration of the NO conversion associated with depletion of the NH_3 surface "reservoir," but fails to account for the maximum in the deNOx rate at decreasing ammonia coverage. In fact, as in the case of ER kinetics, the derivation of the modified θ_{NH_3} rate expression did not consider the ammonia inhibition effect.

3. Modified Redox (MR) Kinetics. In the following we present the full derivation of a new SCR kinetic model. It represents an upgraded and generalized version of a rate expression first reported in Tronconi et al.[29]

It is assumed that two different types of sites are available on the surface of the V_2O_5–WO_3/TiO_2 catalyst: one redox site for O_2 and NO adsorption/reaction (S_1) and one acidic site for NH_3 adsorption (S_2). Kapteijn et al.[21] and Valdés-Solìs et al.[16,17] also reported similar assumptions to derive SCR rate expressions for Mn_2O_3–WO_3/Al_2O_3 catalysts and for carbon-supported V_2O_5 catalysts, respectively.

Even if not strictly relevant for kinetic purposes, in agreement with spectroscopic and mechanistic evidence,[7-12] it can be proposed that S_1 sites are associated with vanadyl species, whereas S_2 sites are associated with other nonreducible, strongly acidic surface sites, such as vanadium-related Brønsted or Lewis sites, or also with sites related to the other oxide catalyst components: it is well known in fact that NH_3 adsorption also occurs on V-free WO_3/TiO_2 catalysts[41] and that these NH_3 adspecies can act as a "reservoir" for NH_3 storage/reaction, as also implied in the Mθ rate law[13] previously discussed.

Starting from oxidized S_1 sites, we propose the following modified redox (MR) kinetic scheme:

Step 1. $S_1{=}O + NO \Leftrightarrow S_1{=}O[NO]$

Step 2. $S_2 + NH_3 \Leftrightarrow S_2[NH_3]$

Step 3. $S_1{=}O[NO] + S_2[NH_3] \rightarrow N_2 + H_2O + S_1{-}OH + S_2$

Step 4. $S_1{-}OH + \frac{1}{4}O_2 \rightarrow S_1{=}O + \frac{1}{2}H_2O$

Step 1 accounts for a weak NO adsorption, Step 2 is the strong ammonia adsorption, the deNOx Step 3 involves reduction of the S_1 sites, and reoxidation of reduced S_1 sites by gaseous oxygen is represented by Step 4.

In addition to Steps 1–4, we further assume the following reversible "NH_3 spillover" step involving adjacent S_1 and S_2 sites:

Step 5. $S_1 + S_2[NH_3] \Leftrightarrow S_1[NH_3] + S_2$

When proceeding to the right, Step 5 results in NH_3 blocking sites S_1, which are thus subtracted from the redox cycle. Accordingly, Step 5 can in principle account for the observed ammonia inhibition.

The overall balances of S_1 and S_2 sites yield

$$1 = \sigma_O + \sigma_{NO} + \sigma_{NH_3} + \sigma_{OH} \tag{10}$$

$$1 = \theta_{free} + \theta_{NH_3} \tag{11}$$

where the terms in the right-hand side of Eq. 10 represent the fractional coverages of $S_1{=}O$, $S_1{=}O[NO]$, $S_1[NH_3]$, and $S_1{-}OH$, respectively, whereas θ_{NH_3} in Eq. 11 indicates the fractional coverage of $S_2[NH_3]$.

We now express the rates of Step 3, that is, the surface reaction between activated NO and adsorbed NH_3, involving reduction of S_1 sites, and of Step 4, involving reoxidation of S_1 sites, as, respectively,

$$r_{NO} = k_{NO}K_{NO}C_{NO}\theta_{NH_3}\sigma_O \tag{12}$$

$$r_{reox} = k_{reox}p_{O_2}^{1/4}\sigma_{OH} \tag{13}$$

Equation 12 implies assuming quasi-equilibrium for Step 1.

By imposition that $r_{NO} = r_{reox}$, we obtain the following relationship between the surface concentrations of reduced and oxidized S_1 sites:

$$\sigma_{OH} = \frac{k_{NO}K_{NO}C_{NO}\theta_{NH_3}}{k_{reox}p_{O_2}^{1/4}}\sigma_O \tag{14}$$

Thus, from Eq. 10 on further assuming negligible surface concentration of NO given its weak adsorption,

$$\sigma_O = \frac{1 - \sigma_{NH_3}}{1 + \dfrac{k_{NO}K_{NO}C_{NO}\theta_{NH_3}}{k_{reox}p_{O_2}^{1/4}}} \tag{15}$$

and, from Eq. 12,

$$r_{NO} = \frac{k^\circ_{NO}e^{-E^\circ_{NO}/RT}C_{NO}\theta_{NH_3}}{1 + k_{O_2}\dfrac{C_{NO}\theta_{NH_3}}{p_{O_2}^{1/4}}}(1 - \sigma_{NH_3}) \tag{16}$$

where $k^\circ_{NO}e^{-E^\circ_{NO}/RT} = k_{NO}K_{NO}$ and $k_{O_2} = k_{NO}K_{NO}/k_{reox}$.

To arrive at a closed form for the deNOx rate equation we still have to evaluate σ_{NH_3}. If we make the general assumption that the rate of NH_3 spillover, Step 5, may be of the same order of magnitude as the rate of NH_3 buildup/depletion on S_2 sites, which determines the characteristic time for the SCR transients, we must take a kinetic approach and write the following balance, for instance, for the S_1-NH_3 sites:

$$\frac{d\sigma_{NH_3}}{dt} = k_{sp}\left[\theta_{NH_3}(1 - \sigma_{NH_3}) - \frac{\sigma_{NH_3}(1 - \theta_{NH_3})}{K_{NH_3}}\right] \tag{17}$$

where K_{NH_3} represents the equilibrium constant of Step 5 above.

The evaluation of the SCR rate r_{NO} according to Eq. 16 then requires time integration of Eq. 17.

A global multiresponse nonlinear regression was performed to fit Eqs. 16 and 17 to all the TRM and TPR runs performed in this work. Notably, because Eq. 16 includes an explicit kinetic dependency on oxygen, data at both 2 and 6% v/v O_2 feed content were included in the regression, in this case for a total of ten transient runs. The temperature dependency of k_{O_2}, K_{NH_3}, and k_{sp} was neglected in the regression to minimize the number of parameters, and a reparameterized form of Eq. 16 was used to reduce correlations among the parameter estimates. The resulting estimates of the five rate parameters (k°_{NO}, E°_{NO}, K_{NH_3}, k_{O_2}, k_{sp}) are listed in Table 1.

Figure 1C (solid lines) illustrates the adequacy of the global fit of the TRM runs with 2% O_2: the MR rate law can evidently capture the complex maxima–minima features of the experimental NO and N_2 traces (symbols) at low T at both NH_3 start-up and shutdown much better than Eq. 8 (Figure 1A, solid lines) and Eq. 9 (Figure 1B, solid lines).

The parameter estimates provided by the fit based on MR kinetics were also used to simulate the experiments of Figure 2, that is, the fast ammonia pulses, which are particularly demanding with respect to the ammonia inhibition effect. Such simulation results are also displayed in Figure 2 (solid lines): it is apparent that, on a purely predictive basis, the MR rate expression is able to follow the fast transients of these experiments. On the other hand, neither the simple Eley–Rideal kinetics (not reported) nor the modified θ_{NH_3} kinetics (Mθ) (see Figure 5) were able to successfully simulate the same experimental transients. Indeed, as seen already in Figure 1, only the MR rate expression is able to correctly account for the maxima–minima features of the NO and N_2 traces related to the NH_3-inhibiting effect.

It is worth mentioning that a simplified, closed rate expression can be readily obtained from Eq. 16 under the limiting assumption of fast NH_3 spillover: in line with this hypothesis, in fact, we can invoke quasi-equilibrium for Step 5 to derive

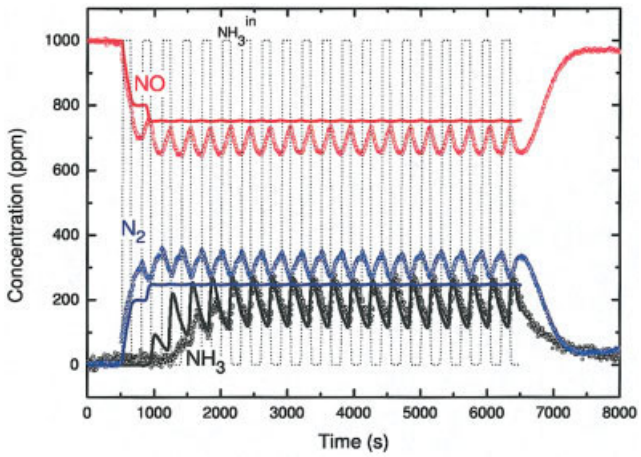

Figure 5. Transient SCR microreactor experiments with high-frequency NH_3 feed pulses.

Data as in Figure 2. Solid lines: simulation using the modified θ_{NH_3} rate law (Eq. 9). [Color figure can be viewed in the online issue, which is available at www.interscience.wiley.com]

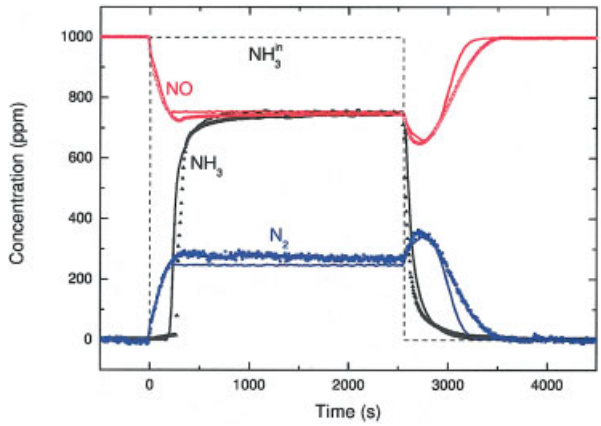

Figure 6. Transient SCR microreactor experiment with step feed of NH_3 (0–1000 ppm) in NO (1000 ppm) + O_2 (2% v/v) and H_2O (1% v/v) + He at 200°C.

Symbols: measured concentrations of NH_3, NO, and N_2 at reactor outlet. Lines: kinetic fit using Eq. 19. [Color figure can be viewed in the online issue, which is available at www.interscience.wiley.com]

$$1 - \sigma_{NH_3} = \frac{1}{1 + K_{NH_3}\dfrac{\theta_{NH_3}}{1 - \theta_{NH_3}}} \tag{18}$$

By substituting Eq. 18 into Eq. 16, we then arrive at the following explicit form of the redox SCR rate equation:

$$r_{NO} = \frac{k^\circ_{NO} e^{-E^\circ_{NO}/RT} C_{NO}\theta_{NH_3}}{\left(1 + K_{NH_3}\dfrac{\theta_{NH_3}}{1 - \theta_{NH_3}}\right)\left(1 + k_{O_2}\dfrac{C_{NO}\theta_{NH_3}}{p_{O_2}^{1/4}}\right)} \tag{19}$$

Equation 19 involves one adjustable parameter less than the general form of Eqs. 16 and 17. It was also fitted to the ten transient TRM and TPR runs at 2 and 6% O_2. The fit results were essentially identical to those reported in Figure 1C, except for the small transient features observed during ammonia step feed to the reactor in the low-T TRM runs, which were not reproduced by Eq. 19. As an example, the comparison between the model fit based on Eq. 19 and the experimental data for the TRM run with 2% oxygen at 200°C is illustrated in Figure 6.

Kinetic effect of oxygen

The MR rate model (Eqs. 16 and 17 or Eq. 19) relies on the assumption that the SCR reaction is governed by a redox mechanism and therefore predicts a kinetic dependency on oxygen, so it was further validated against the experimental data collected at the higher oxygen content. Figures 3 and 4 compare model predictions (solid lines) obtained using the MR rate law with the corresponding experimental results (symbols) obtained performing TRM runs at different temperatures in the presence of 6% v/v of oxygen and TPR runs with either 2 or 6% v/v oxygen in the feed stream, respectively. Inspection of Figures 3 and 4 confirms that changing the deNOx rate law from the ER-based Eqs. 8 and 9 to the new MR kinetic model,

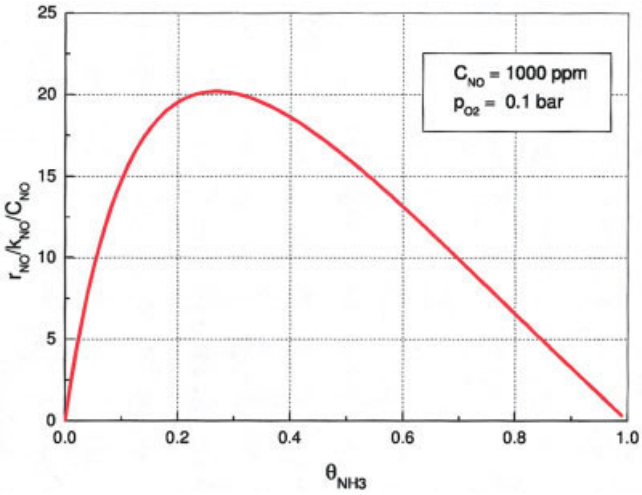

Figure 7. θ dependency of MR rate law (Eq. 19).

p_{O2} = 0.1 bar and C_{NO} = 1000 ppm. [Color figure can be viewed in the online issue, which is available at www.interscience.wiley.com]

Eqs. 16 and 17, not only brings about a remarkable improvement in the description of fast SCR transients, as already apparent from Figures 1 and 2, but also allows a good description of the experimental oxygen effect.

Analysis of the MR rate law

Equations 16 and 17 (or their simplified form Eq. 19) have specific implications with respect to important SCR kinetic and mechanistic issues. Herein we discuss such implications in relation to Eq. 19 for the sake of simplicity, but the following considerations apply as well to the more general form, Eqs. 16 and 17.

The MR rate expression Eq. 19 differs from the Eley–Rideal rate Eq. 8 only in its denominator, which accounts both for the adverse kinetic effect of NH_3 and for the favorable O_2 dependency: at low ammonia coverages (such as at high temperature), the denominator tends to unity and Eq. 19 formally reduces to Eq. 8. Indeed, this is consistent with experimental indications discussed in previous sections: the ammonia-inhibiting effect is particularly evident at low temperatures, but tends to disappear in the runs performed at temperatures $\geq$ 250°C, where ammonia coverages become lower. The oxygen dependency is likewise most manifest at low temperatures according to the SCR literature[6]; however, this is less clearly obvious from the data reported herein, given that complete NO conversion was already approached at $T > 275$°C under our experimental conditions.

The improved transient kinetic fit associated with MR kinetics originates from the capability of Eq. 19 to accommodate the NH_3 inhibition effects, which indicate the existence of optimal ammonia surface concentrations. This can be better focused by analyzing the dependency of Eq. 19 on the ammonia coverage θ_{NH_3}. In Figure 7, calculated values of $r_{NO}/k_{NO}/C_{NO}$ are plotted as a function of θ_{NH_3} for p_{O_2} = 0.1 bar and C_{NO} = 1000 ppm: a maximum in the SCR reaction rate is apparent at $\theta_{NH_3} \approx$ 0.28, the optimal coverage actually depending on reaction conditions. Thus, the deNOx efficiency is enhanced if the mean ammonia coverage is brought close to its optimal value, which can be predicted by Eq. 19: this observation, of course, has important consequences for the rational selection of the urea-injection strategy in SCR systems for vehicles.

With respect to NH_3 inhibition, we further remark that the transient effects observed at low temperature during the NH_3 shutdown phase exhibit characteristic times of a few minutes (see Figures 1 and 3); that is, they are of the same order of magnitude as the characteristic times for buildup/depletion of ammonia adsorbed onto the SCR catalyst. This is consistent with Step 5 in the derivation of the MR kinetic model, which attributes the blocking of the active sites S_1 to spillover of ammonia already adsorbed onto S_2 sites.

The derivation of the simplified MR rate law (Eq. 19) assumed quasi-equilibrium for Step 5, that is the NH_3 spillover step, thus meaning that as soon as ammonia is adsorbed onto S_2 sites it can spill to adjacent S_1 redox sites. This would imply that S_1 and S_2 sites are characterized by a similar NH_3 adsorption capability. Indeed, it is reported[40] that ammonia can adsorb onto all the different types of sites (vanadia, tunsgta, and titania) that are characterized by different acidities, however; more specifically, the most acidic sites are known to be tungsta and titania, whereas vanadia, also because of the fact that is present in smaller amount, participates in a limited way to determine the overall ammonia adsorption capacity. Considering also that S_1 sites may be associated with vanadyl species, whereas the S_2 sites are likely associated with the other acidic surface sites, it appears that the quasi-equilibrium assumption for Step 5 may not be totally consistent in principle with the physicochemical properties of V/W/Ti catalysts. According to a more plausible picture, as soon as it is admitted to the reactor ammonia starts adsorbing onto the more acidic and more abundant S_2 sites: when the catalyst is close to saturation, ammonia is partially transferred to the less acidic and less abundant S_1 sites and blocks them, thus inhibiting the SCR reaction. Accordingly, the spillover Step 5 is likely a slow, activated, kinetically controlled process, in line with the better description of the low-T transients at ammonia step feed provided by Eq. 16. Nevertheless, the quasi-equilibrium assumption for Step 5 in Eq. 19 seems to grant an excellent approximation for practical and engineering purposes, as apparent from Figure 6.

As a final remark concerning ammonia inhibition, whereas in the present MR rate model this kinetic effect is represented by NH_3 directly blocking the catalyst redox sites, other physicochemical interpretations cannot be ruled out, such as adsorbed ammonia adversely affecting the redox properties of the S_1 sites by electronic interaction, as mentioned in a previous section: more fundamental work in this direction would be needed to discriminate. Should the alternative hypothesis be true, however, the MR rate proposed herein could still be regarded as an effective model describing the influence of adsorbed ammonia on the rate constants of the deNOx Steps 3 and 4.

Interestingly, the MR rate model (Eq. 19) also predicts that the apparent kinetic order of NO may be less than unity at large NH_3 coverages. This is in line with the results of Baiker et al.,[14,15] who invoked both a Langmuir–Hinshelwood (LH) mechanism at low temperature and an Eley–Rideal (ER) mechanism at high temperature to fit their SCR kinetic data: the present MR rate model unifies two such asymptotes within a single kinetic scheme. It is worth emphasizing, however, that according to the present approach the nonlinear rate depen-

dency on NO results from a Mars–van Krevelen type mechanism, rather than from competitive adsorption of NO with oxygen, as implied by the LH scheme proposed in Roduit et al.[15]

Indeed, only weak NO adsorption has been assumed in the derivation of Eq. 19: it is worth emphasizing that the MR rate model does not explain NH_3 inhibition by competitive adsorption between NO and NH_3, but rather by ammonia subtracting part of the active catalyst sites from the redox cycle. Therefore, this deactivation mechanism applies irrespective of whether NO, NH_3, or both are activated by the V-related catalyst centers. In this respect, dedicated experiments (not reported) have clearly indicated that the same catalyst of the present study, previously oxidized, is reduced at 200 °C by neither ammonia nor nitric oxide alone; on the other hand, it is effectively reduced when cofeeding the two species together.

As presented in detail elsewhere,[23,29] a fully transient two-phase 1D + 1D model of the SCR monolithic converter incorporating a simplified form of Eq. 19 has been successfully validated in engine test bench runs, accurately predicting the performances of full-scale SCR converters during ESC and ETC test cycles with real exhaust gases from diesel engines, the deviations between simulated NOx conversions and experimental data being typically <4%.

Conclusions

Transient kinetic methods indicate that conventional or modified Eley–Rideal approaches, successfully used in the past to fit deNOx-SCR data for stationary applications, are inadequate to represent the NH_3-SCR dynamics over V_2O_5–WO_3/TiO_2 catalysts in the low-temperature region, which is quite important for automotive applications.

Although more fundamental work is needed to discriminate among possible rival mechanistic interpretations, we have shown that an original kinetic model of the SCR reaction relying on a dual-site modified redox (MR) approach is compatible with the ammonia-inhibition effects observed during unsteady SCR experiments, as well as with the oxygen dependency of the SCR kinetics at low temperatures, and can be successfully applied to simulate the complex dynamic behavior of real exhaust gas aftertreatment systems for vehicles.

The new redox rate model predicts the existence of an optimal ammonia surface coverage at low temperatures, but reduces to the well-established Eley–Rideal form at T≥250°C, that is, in the range of temperatures typical of SCR stationary applications.

The MR rate law has been derived assuming that: (1) two types of sites for NH_3 adsorption (acidic nonreducible sites) and for NO + NH_3 activation/reaction (redox sites), respectively, prevail on the catalyst surface; (2) NH_3 blocks the redox sites; and (3) reoxidation of the redox sites is rate controlling. Each of these assumptions is consistent either with mechanistic evidence available in the SCR literature or with experimental evidence from this work. Of course, goodness of fit cannot be taken as a conclusive proof in favor of a proposed kinetic mechanism, and dedicated research based on spectroscopic measurements would be required at this scope. However, the fact that the MR rate law does a better job than Eley–Rideal approaches in reproducing transient SCR data suggests that, in view of mobile applications, more insight is needed into the mechanism and kinetics of this process than available from previous investigations of SCR catalysis over V-based systems for stationary applications, specifically in the area of low temperatures ($T < 250$°C).

Acknowledgments

Critical suggestions by Professor Pio Forzatti are gratefully acknowledged.

Notation

C_i = gas-phase concentration of species i, mol/m$^3_{gas}$
E°_{des} = activation energy for NH_3 desorption at zero-coverage, kcal/mol
E°_{NO} = activation energy for the deNOx reaction, kcal/mol
E_{ox} = activation energy for NH3 oxidation, kcal/mol
k°_{NO} = preexponential factor for the deNOx reaction rate constant, m^3 mol^{-1} s^{-1}
K_{NO} = adsorption constant for NO, m^3/mol
k°_{ox} = preexponential factor for NH_3 oxidation rate constant, 1/s
k_{ads} = rate constant for NH3 adsorption, 1/s
k°_{des} = preexponential factor for NH_3 desorption rate, m^3 mol^{-1} s^{-1}
k_{ox} = rate constant for NH3 oxidation, m^3 mol^{-1} s^{-1}
k_{reox} = rate constant for catalyst reoxidation, m^3 mol^{-1} bar$^{-1/4}$ s^{-1}
k_{sp} = rate constant for NH3 spillover, 1/s
p_{O_2} = oxygen partial pressure, bar
R = ideal gas constant, cal mol^{-1} K^{-1}
r_{ads} = rate of NH3 adsorption, 1/s
r_{des} = rate of NH3 desorption, 1/s
r_{NO} = rate of deNOx reaction, 1/s
r_{ox} = rate of NH3 oxidation, 1/s
T = temperature, K
t = time, s
v = gas linear velocity, m/s
z = reactor axial coordinate, m

Greek letters

α = parameter for surface coverage dependency
β = O_2 reaction order in NH_3 oxidation rate law
ε = void fraction of catalyst bed
θ_{NH_3} = NH_3 surface coverage
$\theta^*_{NH_3}$ = critical NH_3 surface coverage in Mθ rate law
Ω = catalyst NH_3 adsorption capacity, mol/m$^3_{cat}$

Literature Cited

1. European Automobile Manufacturers Association (ACEA). Final report on selective catalytic reduction; June 2003. Available at http://europa.eu.int/comm/enterprise/automotive/mveg_meetings/meeting94/scr_paper_final.pdf
2. Koebel M, Elsener M, Kleemann M. Urea-SCR: A promising technique to reduce NOx emissions from automotive diesel engines. *Catal Today.* 2000;59:335-345.
3. Heck RM, Farrauto RJ, Gulati ST. *Catalytic Air Pollution Control*. Second Edition. New York, NY: Wiley; 2002.
4. Cross-Cut Lean Exhaust Emissions Reduction Simulations (CLEERS), Knoxville, TN; www.cleers-org
5. Forzatti P, Lietti L, Tronconi E. Nitrogen oxides removal—Industrial. In Horvath IT, ed. *Encyclopedia of Catalysis*. First Edition. New York, NY: Wiley; 2002 (see references contained therein).
6. Busca G, Lietti L, Ramis G, Berti F. Chemical and mechanistic aspects of the selective catalytic reduction of NO_x by ammonia over oxide catalysts: A review. *Appl Catal B Environ.* 1998;18:1-36 (see references contained therein).
7. Dumesic JA, Topsøe N-Y, Slabiak T, Morsing P, Clausen BS, Tornqvist E, Topsøe H. New frontiers in catalysis. In Guczi L, Solymosi F, Tetenyi P, eds. *Proceedings of the 10th International Congress on Catalysis, Budapest*. Budapest, Hungary: Akadémiai Kiadò; 1993:1325.
8. Topsøe N-Y, Topsøe H. Mechanism of the selective catalytic reduction

of nitric-oxide by ammonia elucidated by in-situ online Fourier-transform infrared-spectroscopy. *Science.* 1994;265:1217.
9. Topsøe N-Y, Topsøe H, Dumesic JA. Vanadia/titania catalysts for selective catalytic reduction (SCR) of nitric oxide by ammonia. I. *J Catal.* 1995;151:226-240.
10. Topsøe N-Y, Dumesic JA, Topsøe H. Vanadia/titania catalysts for selective catalytic reduction (SCR) of nitric oxide by ammonia. II. *J Catal.* 1995;151:241-252.
11. Dumesic JA, Topsøe N-Y, Topsøe H, Chen Y, Slabiak T. Kinetics of selective catalytic reduction of nitric oxide by ammonia over vanadia/titania. *J Catal.* 1996;163:409-417.
12. Wachs IE, Deo G, Weckhuysen BM, Andreini A, Vuurman MA, de Boer M, Amiridis MD. Selective catalytic reduction of NO with NH_3 over supported vanadia catalysts. *J Catal.* 1996;161:211-221.
13. Lietti L, Nova I, Camurri S, Tronconi E, Forzatti P. Dynamics of the SCR-deNOx reaction by the transient-response method. *AIChE J.* 1997;43:2559-2570.
14. Willi R, Roduit B, Koeppel RA, Wokaun A, Baiker A. Selective catalytic reduction of NO by NH_3 over vanadia-based commercial catalyst: Parametric sensitivity and kinetic modelling. *Chem Eng Sci.* 1996;51:2897-2902.
15. Roduit B, Wokaun A, Baiker A. Global kinetic modeling of reactions occurring during selective catalytic reduction of NO by NH_3 over vanadia/titania-based catalysts. *Ind Eng Chem Res.* 1998;37:4577-4590.
16. Valdés-Solìs T, Marban G, Fuertes AB. Low-temperature SCR of NO_x with NH_3 over carbon-ceramic supported catalysts. *Appl Catal B Environ.* 2003;46:261-271.
17. Valdés-Solìs T, Marban G, Fuertes AB. Kinetics and mechanism of low-temperature SCR of NO_x with NH_3 over vanadium oxide supported on carbon-ceramic cellular monoliths. *Ind Eng Chem Res.* 2004;43:2349-2355.
18. Willey RJ, Elridge JW, Kittrell JR. Mechanistic model of the selective catalytic reduction of nitric oxide with ammonia. *Ind Eng Chem Prod Res Dev.* 1985;24:226-233.
19. Willey RJ, Lai H, Peri JB. Investigation of iron oxide-chromia-alumina aerogels for the selective catalytic reduction of nitric oxide by ammonia. *J Catal.* 1991;130:319-331.
20. Kapteijn F, Singoredjo L, Dekker NJJ, Moulijn JA. Kinetics of the selective catalytic reduction of nitrogen oxide (NO) with ammonia over Mn_2O_3-WO_3/γ-Al_2O_3. *Ind Eng Chem Res.* 1993;32:445-452.
21. Koebel M, Elsener M. Selective catalytic reduction of NO over commercial deNO_x-catalysts: Experimental determination of kinetic and thermodynamic parameters. *Chem Eng Sci.* 1998;53:657-669.
22. Nova I, Lietti L, Tronconi E, Forzatti P. Dynamics of SCR reaction over a TiO_2-supported vanadia–tungsta commercial catalyst. *Catal Today.* 2000;60:73-82.
23. Chatterjee D, Burkhardt T, Bandl-Konrad B, Braun T, Tronconi E, Nova I, Ciardelli C. Numerical simulation of ammonia SCR-catalytic converters: Model development and application. *SAE Technical Paper 2005-01-965*. Society of Automotive Engineers; 2005.
24. Lietti L, Forzatti P. Temperature programmed desorption/reaction of ammonia over V_2O_5/TiO_2 De-No_xing catalysts. *J Catal.* 1994;147:241-249.
25. Lietti L, Forzatti P, Bregani F. Steady-state and transient reactivity study of TiO_2-supported V_2O_5-WO_3 De-NOx catalysts: Relevance of the vanadium–tungsten interaction on the catalytic activity. *Ind Eng Chem Res.* 1996;35:3884-3892.
26. Marshneva VI, Slavinskaya EM, Kalinkina OV, Odegova GV, Moroz EM, Lavrova GV, Salanov AN. The influence of support on the activity of monolayer vanadia-titania catalysts for selective catalytic reduction of NO with ammonia. *J Catal.* 1995;155:171-183.
27. Ciardelli C, Nova I, Tronconi E, Konrad B, Chatterjee D, Ecke K, Weibel M. SCR-deNO_x for diesel engine exhaust aftertreatment: Unsteady-state kinetic study and monolith reactor modelling. *Chem Eng Sci.* 2004;59:5301-5309.
28. Ciardelli C, Nova I, Tronconi E, Chatterjee D, Bandl-Konrad B. A "nitrate route " for the low temperature "fast SCR " reaction over a V_2O_5–WO_3/TiO_2 commercial catalyst. *Chem Commun.* 2004;2718-2719.
29. Tronconi E, Nova I, Ciardelli C, Chatterjee D, Bandl-Konrad B, Burkhardt T. Modelling of an SCR catalytic converter for diesel exhaust after treatment: Dynamic effects at low temperature. *Catal Today.* 2005;105:529-536.
30. Ciardelli C, Nova I, Tronconi E, Bandl-Konrad B, Chatterjee D, Weibel M, Krutzsch B. Reactivity of NO/NO_2-NH_3 SCR systems for diesel exhausts aftertreatment: Identification of the reaction network as a function of temperature and NO_2 feed content. *Appl Catal B Environ.* 2006; in press.
31. Nova I, Ciardelli C, Tronconi E, Chatterjee D, Bandl-Konrad B. NH_3-NO/NO_2 chemistry over V-based catalysts and its role in the mechanism of the fast SCR reaction. *Catal Today.* 2006;114:3-12.
32. Mears DE. Tests for transport limitations in experimental catalytic reactors. *Ind Eng Chem Process Des Dev.* 1971;10:541-547.
33. Donati G, Buzzi-Ferraris G. Powerful method for Hougen–Watson model parameter estimation with integral conversion data. *Chem Eng Sci.* 1974;29:1504-1509.
34. Villa PL, Forzatti P, Buzzi-Ferraris G, Garone G, Pasquon I. Synthesis of alcohols from carbon monoxide and hydrogen. 1. Kinetics of the low-pressure methanol synthesis. *Ind Eng Chem Prod Res Dev.* 1985;24:12-19.
35. Sanchez-Escrivano V, Montanari T, Busca G. Low temperature selective catalytic reduction of NOx by ammonia over H-ZSM-5: An IR study. *Appl Catal B Environ.* 2005;58:19-23.
36. Sun Q, Gao ZX, Chen HY, Sachtler WMH. Reduction of NO_x with ammonia over Fe/MFI: Reaction mechanism based on isotopic labelling. *J Catal.* 2001;201:89-99.
37. Sun Q, Gao ZX, Wen B, Sachtler WMH. Spectroscopic evidence for a nitrite intermediate in the catalytic reduction of NO_x with ammonia on Fe/MFI. *Catal Lett.* 2002;78:1-5.
38. Andersson LAH, Brandin JGM, Odenbrand CUI. Selective catalytic reduction of NO_x over acid-leached mordenite catalysts. *Catal Today.* 1989;4:173-185.
39. Brandin JGM, Andersson LAH, Odenbrand CUI. Catalytic reduction of nitrogen oxides on mordenite: Some aspects on the mechanism. *Catal Today.* 1989;4:187-203.
40. Wallin M, Karlsson CJ, Palmqvist A, Skoglundh M. Selective catalytic reduction of NO_x over H-ZSM-5 under lean conditions using transient NH_3 supply. *Topics Catal.* 2004;30/31:107-113.
41. Lietti L, Alemany JL, Forzatti P, Busca G, Ramis G, Giamello E, Bregani F. Reactivity of catalysts in the selective catalytic reduction of nitric oxide by ammonia. *Catal Today.* 1996;29:143-148.

Manuscript received Feb. 24, 2006, and revision received May 22, 2006.